Front. Electr. Electron. Eng. China 2007, 2(1): 112–116
DOI 10.1007/s11460-007-0021-z

RESEARCH ARTICLE

WANG Li, YAN Yangguang, CAO Xiaoqing, MENG Xiaoli

Analysis of DC output voltage ripple in an electromagnetic doubly salient brushless DC generator

Abstract Considering the salient pole and high magnetic nonlinearity of the electromagnetic doubly salient (EMDS) DC generator, a 12/8 pole prototype EMDS generator is designed and calculated using a 2-D finite element method (FEM). The phenomenon is analyzed and that the phase voltage wave changes between 120° and 180°. The influence of the exciting current and armature reaction on the DC voltage ripple of the generator is discussed in detail, and the nonlinear rules are gained that DC voltage ripple changes accordingly. The theoretical analysis is verified by the simulation and experimental results. The results are helpful for the optimal design of the generator and the optimal control of exciting-winding. We conclude that the filter-capacitance of the rectifier can be designed.

Keywords electromagnetic, doubly salient generator, FEM, ripple, armature reaction

1 Introduction

An electromagnetic doubly salient motor (EMDSM) is similar to a doubly salient permanent magnet motor (DSPM). The former substitutes the permanent magnet configuration of the latter with an electromagnet [1]. The generator can maintain a constant voltage output by adjusting the exciting current when the load or speed is changed. To produce DC voltage, only a 3-phase rectifying bridge rather than a power converter and rotor position sensor is needed. As a result, compared with an Switch Reluctance Motor (SRM) and a permanent magnet generator [2–4], the EMDSM has a simpler structure and is easier to control. It overcomes the disadvantage of the permanent motor, which is unable to weaken the magnetic-field to adjust the output voltage when a short happens. Moreover, it only needs a simple control and is easily integrated with the bridge rectifier. Therefore, it is quite suitable for use on the main generator of the aviation 270 V high voltage DC power system.

At present, research on the doubly salient motor is mainly concentrated in the linear analysis for the static character of the DSPM [5–9]. On the assumption that the magnetic circuit is unsaturated, Ref. [11] simulates and analyzes the torque ripple of the EMDSM based on a linear model, and presents the method to minimize the torque ripple. Reference [13] calculates and analyzes the EMDSM's static character in a 2-D FEM. The nonlinear model of the EMDSM is built. Due to its salient configuration of the stator and the rotor pole, the doubly salient motor has an obvious edge effect and local saturation, so its air-gap magnetic field distribution is complex and changes cyclically with the rotor angle. As a result, the inductance L and flux linkage ψ are the nonlinear function of the rotor angle θ, the exciting current i_f, the phase current i_a, i_b and i_c. Therefore, the DC output voltage ripple has a certain relation with the exciting current, the phase current and the rotor speed.

The DC voltage ripple is an important parameter in evaluating the quality of the DC generator, so the influence of the exciting current and the armature reaction on a DC voltage ripple of a 12/8 pole EMDS generator is discussed in theory and experiment in this paper. It is assumed that terminal effect is ignored, the magnetic circuit is nonlinear and saturated, and the diodes of the rectifier are ideal without switching time delay. The magnetic field is calculated with a 2-D FEM. Finally, the theoretical analysis is verified by the simulation and experimental results. The results are helpful in the optimal design of the generator and the optimal control of exciting-winding. We conclude that a filter-capacitance of the rectifier can be designed.

2 The EMDSG structure and the analysis method of stable characteristic

The structure of the 12/8 pole EMDSG prototype is shown in Fig. 1. The pole arc width of the stator and the rotor are both at 15°. Suppose the initial position is the position where the

Translated from *Journal of Nanjing University of Aeronautics and Astronautics*, 2006, 38(1): 47–52 [译自: 南京航空航天大学学报]

WANG Li (✉), YAN Yangguang, CAO Xiaoqing, MENG Xiaoli
The Department of Electrical Engineering, Nanjing University of Aeronautics and Astronautics, Nanjing 210016, China
E-mail: Liwang@nuaa.edu.cn

stator tooth of phase B is opposite to the central line of the rotor slot ($\theta = 0°$), and counter-clockwise is the positive rotary orientation.

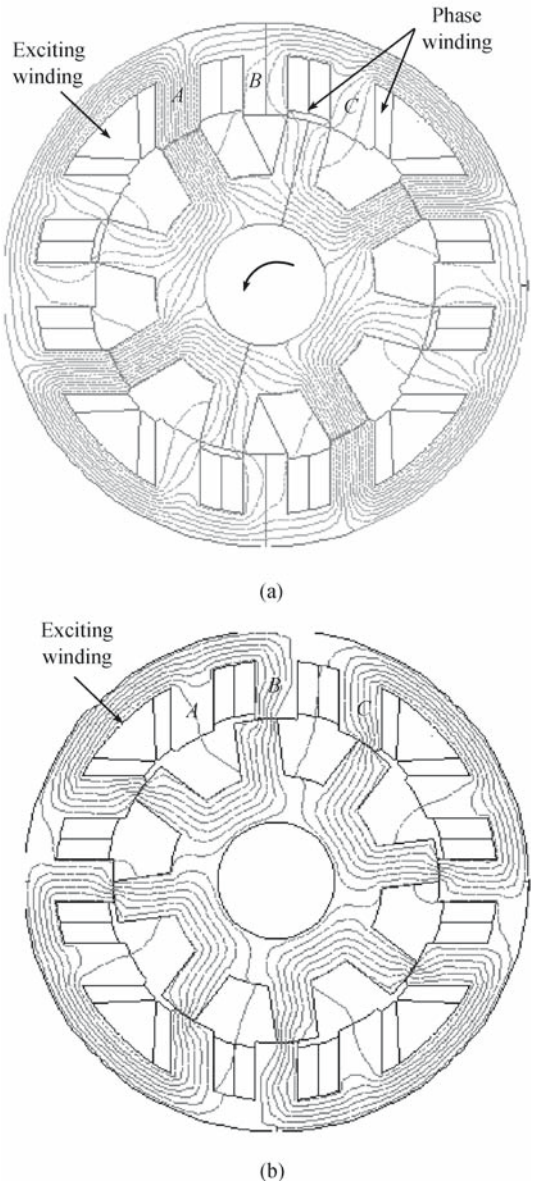

Fig. 1 Flux plot for $i_f = 15$ A 12/8 pole EMDSM at no-load (a) Maximum flux linkage position of the phase A ($\theta = 7.5°$); (b) Minimum flux linkage position of the phase A ($\theta = 30°$)

The voltage equation of the generator is

$$\begin{bmatrix} u_a \\ u_b \\ u_c \\ u_f \end{bmatrix} = \begin{bmatrix} r_a & 0 & 0 & 0 \\ 0 & r_b & 0 & 0 \\ 0 & 0 & r_c & 0 \\ 0 & 0 & 0 & r_f \end{bmatrix} \begin{bmatrix} i_a \\ i_b \\ i_c \\ i_f \end{bmatrix} + \frac{\mathrm{d}}{\mathrm{d}t} \begin{bmatrix} \psi_a \\ \psi_b \\ \psi_c \\ \psi_f \end{bmatrix} \text{ or}$$

$$\boldsymbol{U} = \boldsymbol{R}\boldsymbol{I} + \frac{\mathrm{d}\boldsymbol{\psi}}{\mathrm{d}t} \tag{1}$$

where r_a, r_b, r_c and r_f are phase resistances, ω is angular speed, θ is rotor position and flux linkage is $\boldsymbol{\psi}$ the function of the rotor position and the phase current. The three-phase coils of the EMDS generator are interconnected to form a Y connection. The generator outputs a DC voltage through a three-phase full-bridge commutation. The analytic approach and the equivalent magnetic circuit method are both difficult to gain better results in calculating the generator's characteristic and magnetic field.

The following analysis is based on the fact that the full bridge commutator is ideal and we also ignore the influence of the inductance in the generator. Under this condition, when the generator is working at an actual stable state, it's sure that there will be two phases to output the current at the same time. What's more, the value of the current is the same while the direction is opposite. As a result, the current in the third phase is zero. According to the above analysis, the voltage equation is concluded as

$$\begin{cases} \dfrac{\mathrm{d}(\psi_a - \psi_b)}{\mathrm{d}\theta} = \dfrac{-i_a}{\omega}(r_a + r_b + R_\mathrm{L}) & \theta_1 \leqslant \theta \leqslant \theta_2 \\ \dfrac{\mathrm{d}(\psi_b - \psi_c)}{\mathrm{d}\theta} = \dfrac{-i_b}{\omega}(r_b + r_c + R_\mathrm{L}) & \theta_2 \leqslant \theta \leqslant \theta_3 \\ \dfrac{\mathrm{d}(\psi_c - \psi_a)}{\mathrm{d}\theta} = \dfrac{-i_c}{\omega}(r_c + r_a + R_\mathrm{L}) & \theta_3 \leqslant \theta \leqslant \theta_1 + \dfrac{\pi}{4} \end{cases} \tag{2}$$

where θ_1, θ_2, θ_3 are phase changing angles; r_a, r_b and r_c are phase resistance, R_L is load resistance. Equation (2) is a nonlinear differential equation, so it can be solved by the fourth-order Runge-Kutta method, as in Eq. (3).

$$\begin{cases} \psi_{n+1} = \psi_n + \dfrac{h}{6}\left(K_1 + 2K_2 + 2K_3 + K_4\right) \\ K_1 = \psi(\theta_n, i_n) \\ K_2 = \psi\left(\theta_n + \dfrac{h}{2},\ i_n + \dfrac{h}{2}K_1\right) \\ K_3 = \psi\left(\theta_n + \dfrac{h}{2},\ i_n + \dfrac{h}{2}K_2\right) \\ K_4 = \psi\left(\theta_n + h,\ i_n + hK_3\right) \quad n = 0,1,... \end{cases} \tag{3}$$

where h is step length, $\theta_{n+1} = \theta_n + h$, $\psi(\theta, i)$ is obtained by calculating in FEM, and $i(\theta, \psi)$ is developed from $\psi(\theta, i)$. The phase terminal voltage can be easily obtained according to Eq. (1). Based on the above calculation, the influence of the exciting current i_f and load current I, the output voltage ripple is then analyzed by simulation.

3 Analysis of the influence of exciting current on DC output voltage ripple

In the following analysis, the general case is assumed, no load and exciting current ripple is neglected. The back emf of phase A is given as

$$u_a = -\frac{\mathrm{d}\boldsymbol{\psi}}{\mathrm{d}t} = -\omega\frac{\mathrm{d}\boldsymbol{\psi}}{\mathrm{d}\theta} \tag{4}$$

The relative position of the rotor and the stator where the flux linkage of phase A is at maximum and minimum are shown in Fig. 1. The distribution of flux linkage is also shown in Fig. 1.

The flux linkage and the phase voltage varying with the exciting current under a constant speed are shown in Fig. 2. While the exciting current is smaller, the maximum of the flux linkage increases linearly with the increase of the exciting current. However, if the magnetic circuit is saturated, the maximum of the flux linkage will not increase, while the minimum will increase a little. As shown in Fig. 2(b), the wave of the phase voltage approximates the square wave and the wave peak value is small.

The output voltage waveform has three approximate 120° square-wave, so the output DC voltage includes a little ripple. With the exciting current increasing, the waveform of the phase voltage is almost trapezoidal in form. What's more, the peak value increases, and as a result, the ripple of the DC voltage increases. With a further increase of the exciting current, the waveform peak value of the phase voltage is almost invariable after the magnetic circuit is saturated. The phase voltage waveform changes with the minimum of the flux linkage and gradually approximates a sine wave. But the output DC voltage waveform has a six-crest wave, so the ripple of the DC voltage declines. When the rotary speed is 6 000 r/min under a no-load condition, the curve of the output DC voltage ripple and the ripple factor changes with the exciting current as shown in Fig. 3. The results are in accordance with the analytical conclusions hereinbefore. Under

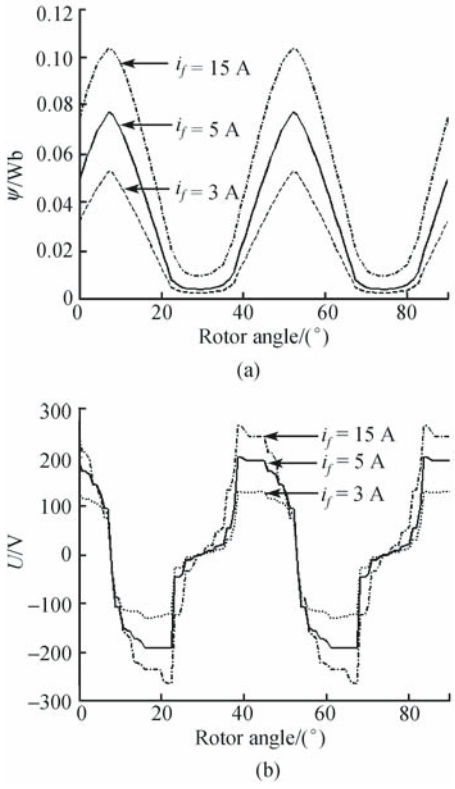

Fig. 2 Phase flux linkage and emf
(a) Flux linkage; (b) Emf

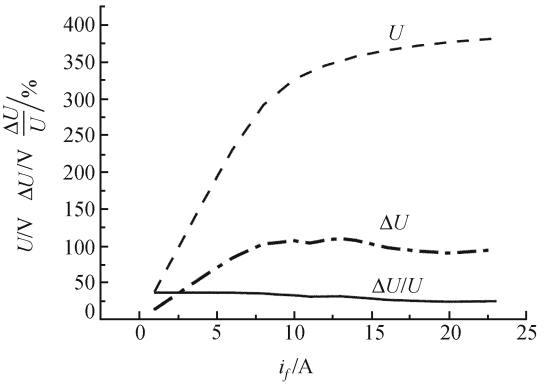

Fig. 3 DC voltage ripple vs. exciting current

ideal circumstances, the ripple of the DC voltage output mainly depends on the waveform shape of the phase voltage and peak value, which depends on the distribution of the magnetic field and the extent of the nonlinear saturation of a magnetic circuit.

4 The analysis of the influence of loading current on output voltage ripple

In the following analysis, on the assumption that the exciting current and the speed is constant and the load is resistance, we define that the direction of the armature current and the emf is identical. Considering the nonlinearity of the magnetic circuit, we analyze the influence of the loading current on the output voltage ripple.

4.1 Analysis constant exciting current and speed

When the speed is 6 000 r/min and the exciting current i_f is 20 A, the simulating waveforms of the flux linkage of phase A and the voltage changing with the position and load current are shown in Fig. 4.

When the exciting current is constant, the waveform of the flux linkage and the phase voltage vary with the changing of position and phase current under the influence of the armature reaction, as shown in Fig. 4. When the rotor rotates counter-clockwise, as shown in Fig. 1(b), the rotor tooth gradually approaches and reaches the stator tooth of phase A; the phase A flux linkage gradually increases up to the maximum. The armature reaction makes the phase flux linkage decrease. The rotor keeps rotating counter-clockwise, the rotor salient pole leaves the stator salient pole, and the armature reaction makes the phase flux linkage increase. When the magnetic circuit is saturated, the armature reaction obviously makes the maximum of the phase flux linkage decrease, as shown in Fig. 4(a). Assuming that the magnetic circuit is saturated under no load, the following load current increases, and the phase voltage waveform changes from sine wave to trapezoidal form, which leads to the DC voltage ripple increasing. When the magnetic circuit is changed from saturated to unsaturated because of the armature reaction decreasing, the phase voltage waveform changes from the trapezoidal form

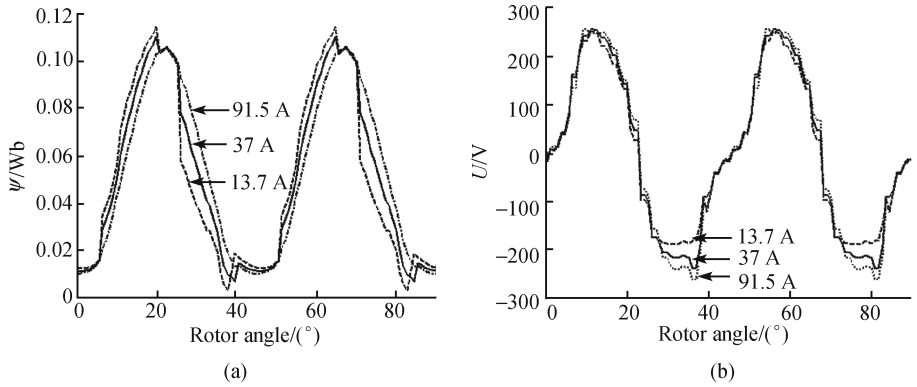

Fig. 4 Flux linkage and phase voltage at different load current ($i_f = 20$ A)
(a) Flux linkage; (b) Phase voltage

to the approximate wave and its peak value is reduced, so that the DC voltage ripple decreases. The larger the exciting current is, the more saturated the magnetic circuit will be. The more the phase current becomes larger, the more the demagnetization effect is distinct.

The DC voltage ripple vs. the load current is shown in Fig. 5. The DC voltage ripple can reach the largest value following an increase in load current. Under a constant load current, the larger the exciting current is, the lower the voltage ripple will be. In conclusion, the voltage ripple at load is higher than at no load because of the effect of the armature reaction. Additionally, the influence of the exciting current ripple is not considered in the analysis above, otherwise the voltage ripple will be higher considering the exciting current ripple.

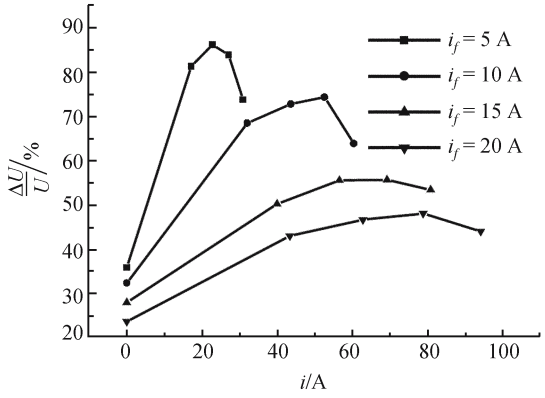

Fig. 5 DC voltage ripple vs. load current at different load current

4.2 The ripple under constant 270 V DC output voltage

Here it is assumed that the speed is constant ($n = 6\,000$ r/min), the load is resistance and the exciting current ripple isn't taken into account. The exciting current must be adjusted to keep the DC voltage output constant at 270 V when the load current is changed. The voltage ripple vs. the load current plots is shown in Fig. 6 based on calculations. The voltage ripple increases to its largest value, then decreases with an increase in the load current. That is because of the effect on armature inductance of armature reaction.

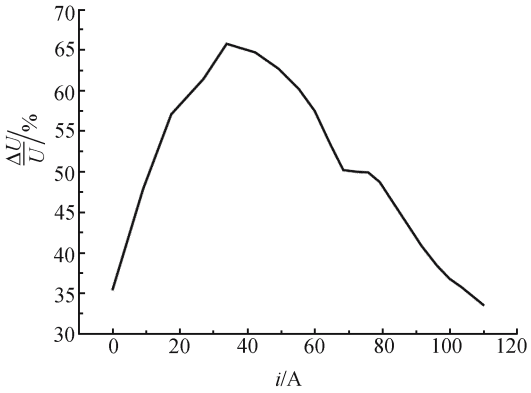

Fig. 6 The simulation curve of DC voltage ripple coefficient vs. load current

5 Experiments

The test is done with a 30 kW 12/8 pole prototype EMDS generator; the results are shown in Figs. 7–9.

The curves of the voltage ripple and the factor varying with the exciting current at no-load and 6 000 r/min are shown in Fig. 7. The voltage ripple at various load current with a 270 V constant DC output voltage is shown in Fig. 8. The result of the test basically coincides with the theoretical analysis.

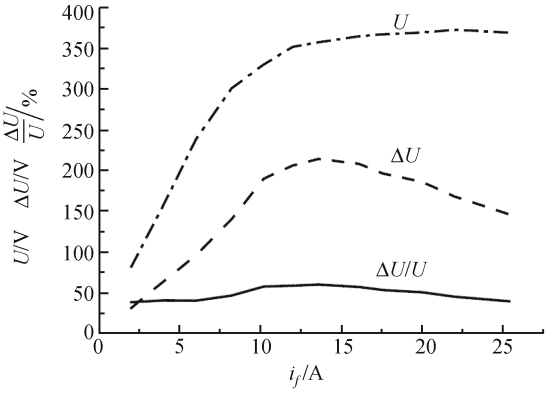

Fig. 7 DC voltage ripple and coefficient vs. exciting current at no load

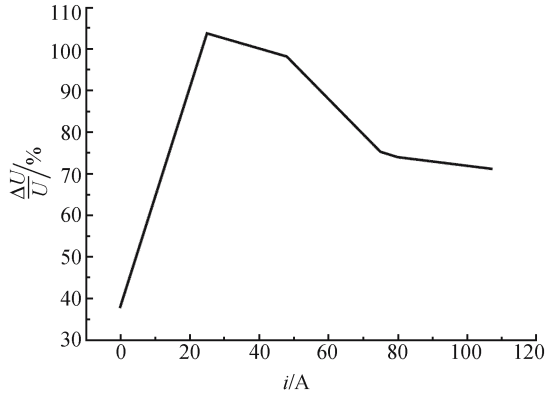

Fig. 8 DC voltage ripple coefficient vs. load current at 270 V

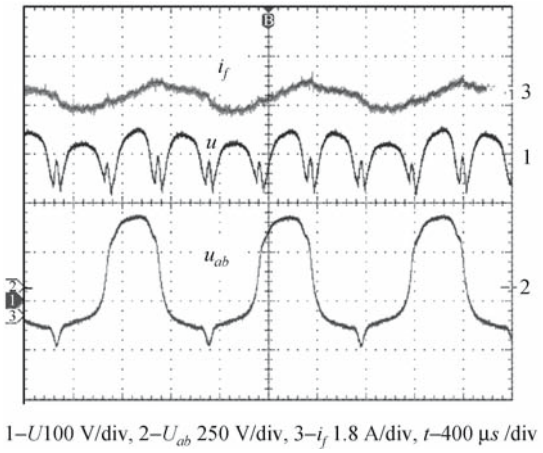

Fig. 9 Test waveform

In comparison with the computed result, the test value of the ripple is larger. Except for the calculation error of the 2-D FEM and modeling, the main reason is that the influence of the exciting current ripple and the current-changing of the commutator isn't considered in the simulation analysis. Figure 9 shows the exciting current waveform at $i_f = 8.2$ A and speed of 6 000 r/min, the ripple frequency is the same as the line voltage (phase voltage) and in direct proportion to the speed. The exciting current ripple is in direct correlation with the structure of the generator, so that the voltage ripple can be decreased by optimizing the structure of the generator, in addition, by a developed exciting control strategy.

6 Conclusions

The influence of the exciting current and the armature reaction on the DC voltage ripple of the generator is discussed in detail by simulation and testing. The conclusions are as follows.

1) At no-load, the voltage ripple increases with the increase of the exciting current and decreases a little when the magnetic circuit is highly saturated. On the condition of a constant load current, the voltage ripple is smaller when the exciting current is larger.

2) On the assumption that the exciting current and the speed are constant and the load is resistance, with the increase of the load current, the DC voltage ripple increases too. The DC voltage ripple can reach its largest value with an increase of the load current. At a constant load current, the larger the exciting current is, the lower the voltage ripple will be. The voltage ripple at a load is higher than at no load because of the effect of the armature reaction. At constant 270 V voltage, the voltage ripple increases to its largest value, then decreases with the increase of the load current.

3) The theoretical analysis is verified by simulation and experimental results. The results are helpful in optimizing the design of a generator and the optimal control of an exciting-winding. We conclude that the filter-capacitance of the rectifier can be designed.

Acknowledgements This work was supported by the National Natural Science Foundation of China (Grant No. 50337030).

References

1. Liu C, Zhou B, Yan Y G. Implementation and study of a novel doubly salient structure starter/generator system. Chinese Journal of Aeronautics, 2002, 15(3): 151–155 (in Chinese)
2. Tomino J, Yosizue K, Chiba A. Output DC voltage control system of a doubly salient-sole homopolar generator. In: Proceeding of the 6th International Workshop on Advanced Motion Control. Nagoya, 2000, 566–571
3. Jahns T M, Caliskan V. Uncontrolled generator operation of interior PM synchronous machines following high-speed inverter shutdown. IEEE Trans. Ind. Appl., 1999, 35(6): 1347–1357
4. Elbaluk M E, Kankam M D. Potential starter/generator technologies for future aerospace application. IEEE AES System Magazine, 1997, 12(5): 24–31
5. Yue Feng, Lipo T A. A new doubly salient permanent magnet motor for adjustable speed driver. Electric Machines and Power Systems, 1994, 22 (2): 258–270
6. Chan K T, Cheng M, Chan C C. Performance analysis of 8/6-pole doubly salient permanent magnet motor. Electric Machines and Power Systems, 1999, 27(10): 1055–1067
7. Cheng M, Chau K T, Chan C C. Static characteristics of a new doubly salient permanent magnet motor. IEEE Transactions on Energy Conversion, 2001, 16(1): 20–25
8. Sun Qiang, Cheng Ming, Zhou E, et al. Analysis of torque ripple in doubly salient permanent magnet motor. Transactions of China Electrotechnical Society, 2002, 17(5): 10–15 (in Chinese)
9. Lin Mingyao, Cheng Ming, Zhou E. Design and analysis of a new 12/8-pole doubly salient permanent-magnet motor. Journal of Southeast University, 2002, 32(6): 944–948 (in Chinese)
10. Zhou Bo, Xiang Rong, Wang Chuanyun. Theoretical analysis on the electromagnetic characteristics for doubly salient electromagnitic machines. ACTA Aeronautic Astronautica Sinica, 2003, 24(4): 355–359 (in Chinese)
11. Xiang Rong, Zhou Bo. Torque-ripple simulation of double salient motor. Journal of Nanjing University of Aeronautics & Astronautics, 2001, 33(4): 366–371 (in Chinese)
12. Cao Fei, Xiang Rong, Zhou Bo. Theory and implement of doubly-salient machine digital control system based on DSP control. Journal of Nanjing University of Aeronautics & Astronautics, 2003, 35(4): 345–250 (in Chinese)
13. Wang Li, Song Xiaofeng, Meng Xiaoli. Nonlinear modeling of fielding-winding doubly salient generator by support vector machine. Transactions of China Electrotechnical Society, 2004, 19(9): 1–5 (in Chinese)